miRNA-145 inhibits myocardial infarction-induced apoptosis through autophagy via Akt3/mTOR signaling pathway *in vitro* and *in vivo*

LIQIU YAN, NAN GUO, YANCHAO CAO, SAITIAN ZENG, JIAWANG WANG, FENGFENG LV, YUNFEI WANG and XUFEN CAO

Department of Cardiology, Cangzhou Central Hospital, Hebei Medical University, Cangzhou, Hebei 061000, P.R. China

Received August 9, 2017; Accepted June 18, 2018

DOI: 10.3892/ijmm.2018.3748

Abstract. The present study investigated the effects of micro (mi)RNA-145 on acute myocardial infarction (AMI) and the potential underlying mechanism. A total of 6 AMI and 6 normal rat tissues were investigated for the present study. It was demonstrated that miRNA-145 expression was downregulated in the AMI rat model, compared with the control group. Downregulation of miRNA-145 increased cardiac cell apoptosis, suppressed phosphorylated (p)-RAC-γ serine/threonine-protein kinase (Akt3) and p-mechanistic target of rapamycin (mTOR) protein expression levels and suppressed autophagy in an *in vitro* model of AMI. However, overexpression of miRNA-145 decreased cardiac cell apoptosis, induced p-Akt3 and p-mTOR protein expression and promoted autophagy in the *in vitro* model of AMI. The inhibition of Akt3 (GSK2110183, 1 nM) decreased the effect of the miRNA-145 upregulation on cell apoptosis in the *in vitro* model of AMI. Chloroquine diphosphate (5 μM) inhibited the regulatory effect of miRNA-145 upregulation on autophagy to adjust cell apoptosis, in the *in vitro* model of AMI. The results of the present study demonstrate that miRNA-145 inhibits myocardial infarction-induced apoptosis via autophagy associated with the Akt3/mTOR signaling pathway *in vivo* and *in vitro*.

Introduction

Cardiovascular disease (CVD) is one of the primary diseases currently threatening human health. In particular, acute myocardial infarction (AMI) is a factor that primarily results in increasing morbidity of CVD patients (1). Therefore, early, timely and accurate diagnosis and evaluation of AMI are essential for actively administrating effective treatment (2). Furthermore, early diagnosis may result in timely cardiac reperfusion and reduce mortality (2). The early treatment of AMI is crucial in the favorable prognosis of patients. At present, creatine kinase isozyme and myoglobin are the predominant serum biomarkers used for the clinical diagnosis of AMI (3). Notably, the aforementioned markers have attained certain levels in sensitivity and specificity of the early diagnosis of AMI (3). However, researchers have continued their efforts in studying novel serum markers with increased sensitivity and specificity (4). Serum markers reflecting the prognosis for AMI patients are of primary research interest (4).

It has previously een demonstrated that non-coding microRNAs (miRNAs) are closely associated with the genesis, development and prognosis of all diseases (5). miRNA expression demonstrates tissue specificity and high stability in the blood (6). Therefore, myocardium specific miRNAs have been speculated to act as ideal biomarkers for the early diagnosis of AMI (5). Furthermore, miRNA is important in numerous pathophysiological processes. These include the genesis and development of Myocardial Infarction (MI), myocardial fibrosis following MI and myocardial remodeling (7). A previous study suggested that miRNA is crucial in the genesis and development of human diseases, including tumor initiation, cardiovascular disease, diabetes, immune system and renal diseases (7). Furthermore, the effects of miRNAs generally manifest as a complicated regulatory network formed by multiple miRNAs during regulation of disease genesis and development (7). Therefore, the study of miRNA is of great importance to the understanding of genesis and developmental mechanisms of various diseases.

Under normal physiological status, the myocardium is energy-supplemented primarily via fat oxidation. However, in the case of an insufficient coronary blood supply, the myocardium is under anoxic conditions (8) and fatty acid oxidation efficiency is low (8). Furthermore, glucose and glycogenolysis for energy supply only account for a small part of aerobic metabolism (9). The persistent ischemia and hypoxia results

Correspondence to: Dr Liqiu Yan, Department of Cardiology, Cangzhou Central Hospital, Hebei Medical University, 16 Xinhua West Road, Cangzhou, Hebei 061000, P.R. China
E-mail: iypn8780888@126.com

Key words: miRNA-145, autophagy, acute myocardial infarction, RAC-γ serine/threonine-protein kinase, mechanistic target of rapamycin

in irreversible mitochondrial injury and myocardial cell death (9). Cell death occurs in three ways: Necrosis, apoptosis and autophagy (10). Apoptosis and autophagy have previously been demonstrated to be involved in ischemia reperfusion injury (10).

The mechanistic target of rapamycin (mTOR) signaling pathway receives and integrates multiple signals (11). These signals include amino acids, glucose, oxidative stress and growth factors (11). Therefore, mTOR exhibits an important regulatory role in cell growth, proliferation, and protein synthesis (12). mTOR signaling has been verified to be one of the canonical autophagy regulatory pathways (13). It is the signaling pathway that senses the cell nutritional status (13) and primarily exerts an autophagy-associated inhibitory effect on cardiac cell apoptosis, whilst stimulating cell growth and proliferation (13).

The phosphoinositide 3-kinase (PI3K)/RAC-γ serine/threonine-protein kinase (Akt)/mTOR signaling pathway exhibits a critical regulatory role in autophagy. A previous study suggests that research has been successful in identifying inhibitory drugs targeting various signaling pathways in order to treat growth of tumors (14). mTOR is the downstream molecule of Akt in the PI3K/Akt regulatory pathway. It is involved in regulating protein synthesis, cell cycle and angiogenesis. PI3K/Akt/mTOR signaling pathway is a core pathway that promotes cell growth, movement, protein synthesis, survival, and hormone, growth factor and nutrient metabolism (15). The present study investigated the effects of miRNA-145 on AMI and the potential underlying mechanism.

Materials and methods

Ethics and AMI model. Adult male Sprague-Dawley (180-220 g; n=12) rats were maintained in cages at 21±2˚C, under a 12 h light-dark cycle, with 55±5% constant humidity, and had free access to food and water. All rats were randomized into two groups: Control (n=10) and AMI model groups (n=10). All animal experimentation was performed in accordance with the NIH Guide for the Care and Use of Laboratory Animals of Cangzhou Central Hospital, Hebei Medical University (Cangzhou, China), and approved by the Ethics Committee of Cangzhou Central Hospital. Rats were anesthetized with pentobarbital sodium (35 mg/kg, i.p.) and exposed following the skin incision in the fourth intercostal space of a left thoracotomy. A snare occlude was used to ligate the left anterior descending coronary artery with 6-0 silk suture. Cardiac ischemia was verified by visual observation and continuous electrocardiogram monitoring. The coronary artery was reperfused by releasing the knot following 1 h of occlusion. A total of 3 h following induction of AMI, cardiac tissue was harvested.

Haematoxylin and eosin (H&E) staining. Cardiac tissue was harvested under pentobarbital sodium (35 mg/kg, i.p.) and washed with PBS. Cardiac tissue was fixed with 4% paraformaldehyde for 24 h and embedded into paraffin. Samples were cut into 4.0 μm of sections and sections were stained with H&E for 5 min at room temperature and observed under a LSM 780 NLO confocal microscope (Carl Zeiss AG, Oberkochen, Germany).

Reverse transcription-quantitative polymerase chain reaction (RT-qPCR) and gene expression microarrays. Total RNA was extracted from tissue samples or cells using TRIzol® kit (Invitrogen; Thermo Fisher Scientific, Inc., Waltham, MA, USA) and total RNA (200 ng) was then reverse transcribed to cDNA using an RT kit (Takara Biotechnology Co., Ltd., Dalian, China). RT-qPCR was performed using SYBR Premix Ex TaqII (Takara Biotechnology Co., Ltd.) and amplification occurred under the following conditions: Pre-denaturation for 10 min at 94˚C; 40 cycles of 30 sec at 94˚C, 30 sec at 55˚C and 30 min at 72˚C, followed by an extension step for 10 min at 72˚C. Primers sequences sued were as follows: miRNA-145 forward, 5'-GGTCCAGTTTTCCCAGG-3' and reverse 5'-CAGTGCGTGTCGTGGAGT-3'; U6 forward, 5'-AGA AGGCTGGGGCTCATTTG-3' and reverse 5'-AGGGGC CATCCACAGTCTTC-3'. Data using RT-qPCR was quantified using the $2^{-\Delta\Delta Cq}$ method (16).

A total of 500 ng total RNA was used to execute the gene expression microarrays, and amplified using the Ovation PicoSL WTA System V2 kit (Nugen Technologies. Inc., CA, USA). cDNA samples were Cy3-labeled using the SureTag DNA labeling kit (Agilent Technologies, Inc., Santa Clara, CA, USA). The scanning was conducted using a SureScan Microarray Scanner and Feature Extraction software, version 10.7.3.1 (Agilent Technologies, Inc.).

Cell culture and cell transfection. The H9c2 cell line was cultured and maintained in Dulbecco's minimum essential medium (DMEM, Thermo Fisher Scientific, Inc.) supplemented with 10% fetal bovine serum (HyClone; GE Healthcare Life Sciences, Logan, UT, USA) at 37˚C, in an environment containing 5% CO_2. 100 ng of miRNA-145 mimics (5'-GUC CAGUUUUCCCAGGAAUCCCU-3'), 100 ng of miRNA-145 inhibitors (5'-AGGGAUUCCUGGGAAAACUGGAC-3') and 100 ng of negative control (5'-CAGUACUUUUGU GUAGUACAA-3') were transfected into H9c2 cells using Lipofectamine 2000 (Thermo Fisher Scientific, Inc) at 37˚C according to the manufacturer's protocol. After transfection for 4 h, old medium was removed and new DMEM was added into H9c2 cells for 20, 44 or 68 h. Then, H9c2 cells were subjected to a hypoxia/reoxygenation protocol for 2 h.

Luciferase reporter gene assay. Bioinformatics software on http://www.targetscan.org was adopted to predict the targeted correlation between miRNA-145 and Akt3. AKT3-3'UTR-WT plasmid and miR-145 mimics were constructed by Shanghai GenePharma, Co., Ltd (Shanghai, China) and transfected using Lipofectamine 2000 (Thermo Fisher Scientific, Inc.). The expression of reporter gene was presented using luminometer reading (TD20/20; Turner Designs, Sunnyvale, CA, USA) by the activity ratio of firefly luciferase and renilla luciferase.

Western blotting. Following cell transfection (n=3) for 48 h, cells were washed with PBS, and total protein was extracted using radioimmunoprecipitation assay lysis buffer (Beyotime Institute of Biotechnology, Nanjing, China), and

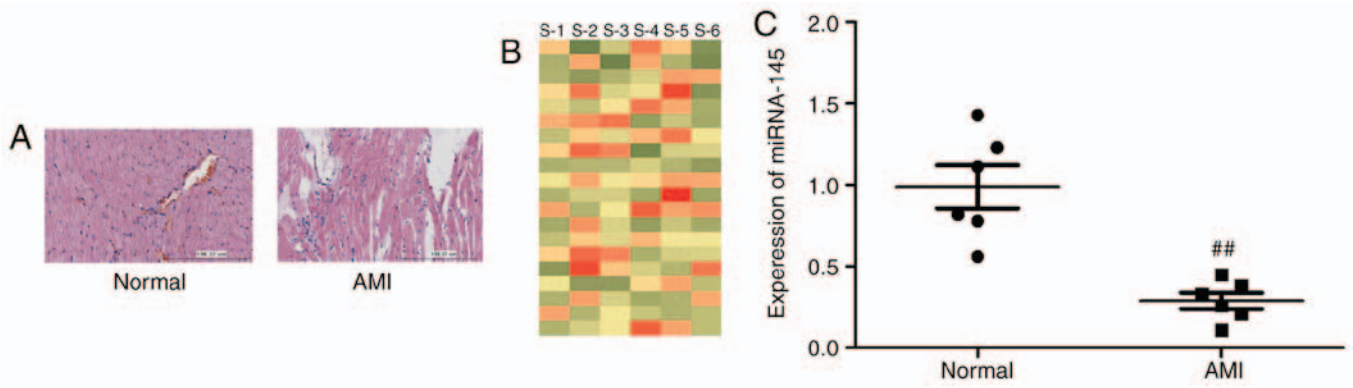

Figure 1. Expression of miRNA-145 in AMI *in vivo* model. (A) Hematoxylin and eosin staining in AMI and normal rat cardiac tissue, magnification x10. (B) Microarray gene chipping for miRNA-145 expression and (C) miRNA-145 expression levels detected via reverse transcription-quantitative polymerase chain reaction. ##P<0.01 vs. control group. miRNA, microRNA; normal, normal control rat group; AMI, acute myocardial infarction rat model group.

then quantified using a bicinchoninic acid assay (Beyotime Institute of Biotechnology). A total of 50 μg total protein was separated by 8-12% sodium dodecyl sulfate polyacrylamide gel electrophoresis (SDS-PAGE) and transferred onto a polyvinylidene fluoride membrane. The membrane was blocked with 5% milk in Tris buffered saline Tween-20 (TBST) and incubated with primary antibodies against B cell lymphoma 2 associated apoptosis regulator (Bax, cat. no. sc-6236; 1:500; Santa Cruz Biotechnology; Inc., Dallas, TX, USA), p-Akt (cat. no. sc-7985-R; 1:500; Santa Cruz Biotechnology; Inc.), p-mTOR (cat. no. sc-101738; 1:500; Santa Cruz Biotechnology; Inc.), microtubule associated protein 1 light chain 3 (LC3, cat. no. sc-292354; 1:500; Santa Cruz Biotechnology; Inc.) and GAPDH (cat. no. sc-25778; 1:500; Santa Cruz Biotechnology; Inc.) at 4˚C overnight. Following this, the membrane was washed with TBST and incubated with goat anti-rabbit IgG-horse radish peroxidase (cat. no. sc-2004; 1:5,000; Santa Cruz Biotechnology; Inc.) for 1 h at 37˚C. Protein bands were exposed by BeyoECL Moon (Beyotime Institute of Biotechnology) and analyzed using Bio-Rad Laboratories Quantity One software, version 3.0 (Bio-Rad Laboratories, Inc., Hercules, CA, USA).

Immunofluorescence. Following cell transfection, (n=3) for 48 h, cells were washed with PBS for 15 min and fixed with 4% paraformaldehyde for 15 min at room temperature. Cells were incubated with 0.1% Triton X-100 for 15 min at room temperature and blocked with 5% bovine serum albumin (Beyotime Institute of Biotechnology) in PBS for 1 h at room temperature and incubated with the primary antibody against LC3 (cat. no. sc-292354; 1:100; Santa Cruz Biotechnology; Inc.), p-Akt (cat. no. sc-7985-R; 1:100; Santa Cruz Biotechnology; Inc.) at 4˚C overnight. Following washing with PBS, cells were incubated in a mixture of fluorescent secondary antibody (Alexa 488 anti-mouse immunoglobulin G; 1:100, cat. no. sc-516248; Santa Cruz Biotechnology; Inc.) for 1 h at room temperature, incubated with DAPI assay for 30 min and analyzed using a LSM 780 NLO confocal microscope (Carl Zeiss AG, Oberkochen, Germany).

MTT assay. Following cell transfection (n=3) for 24, 48 or 72 h, cells were stained with 20 μl MTT (5 g/l, G3582; Promega Corporation, Madison, WI, USA) for 4 h at 37˚C, in an incubator in an environment containing 5% CO_2. A total of 150 μl dimethyl sulfoxide was added to cells and shaken for 10 min. Cell proliferation was measured using a microplate reader (SpectraMax M5; Molecular Devices, LLC, Sunnyvale, CA, USA) at a wavelength of 490 nm.

Flow cytometry. Following cell transfection (n=3) for 48 h at 37˚C, cells (1x10^6 cell/ml) were collected at 1,000 x g for 10 min at 4˚C and washed with PBS, fixed with 4% paraformaldehyde for 15 min at room temperature and resuspended with 150 μl binding buffer. A total of 10 μl Annexin V-FITC and 5 μl propidium iodide (BB-4101-2; BestBio Science., Shanghai, China) staining solution were added to the cells for 15 min, in the dark. Flow cytometry was used to detect cell apoptosis and analyzed using Flowjo 7.6.1 (FlowJo, LLC,).

Statistical analysis. Data are presented as the mean ± standard deviation (n=3) using SPSS software, version 17.0 (SPSS Inc., Chicago, IL, USA), and were analyzed by one-way analysis of variance (ANOVA) or two-way ANOVA followed by Tukey's post-hoc test. P<0.05 was considered to indicate a statistically significant difference.

Results

Expression of miRNA-145 in AMI in vivo model. Firstly, the present study measured the alteration of miRNAs in the AMI *in vivo* model using the microarray gene chip method. As presented in Fig. 1A, H&E staining of heart tissue indicated that there was myocardial damage in the AMI model, compared with normal group. miRNA-145 expression was downregulated in the AMI rat model, compared with control group (Fig. 1B). In addition, miRNA-145 expression was analyzed using RT-qPCR. Fig. 1C demonstrated that miRNA-145 expression was downregulated in the AMI rat model, compared with control group. It was therefore hypothesized that miRNA-145 may be a regulator for AMI.

Downregulation of miRNA-145 increases cardiac cell apoptosis in an in vitro model of AMI. To test the function of miRNA-145 in an *in vitro* model of AMI, the

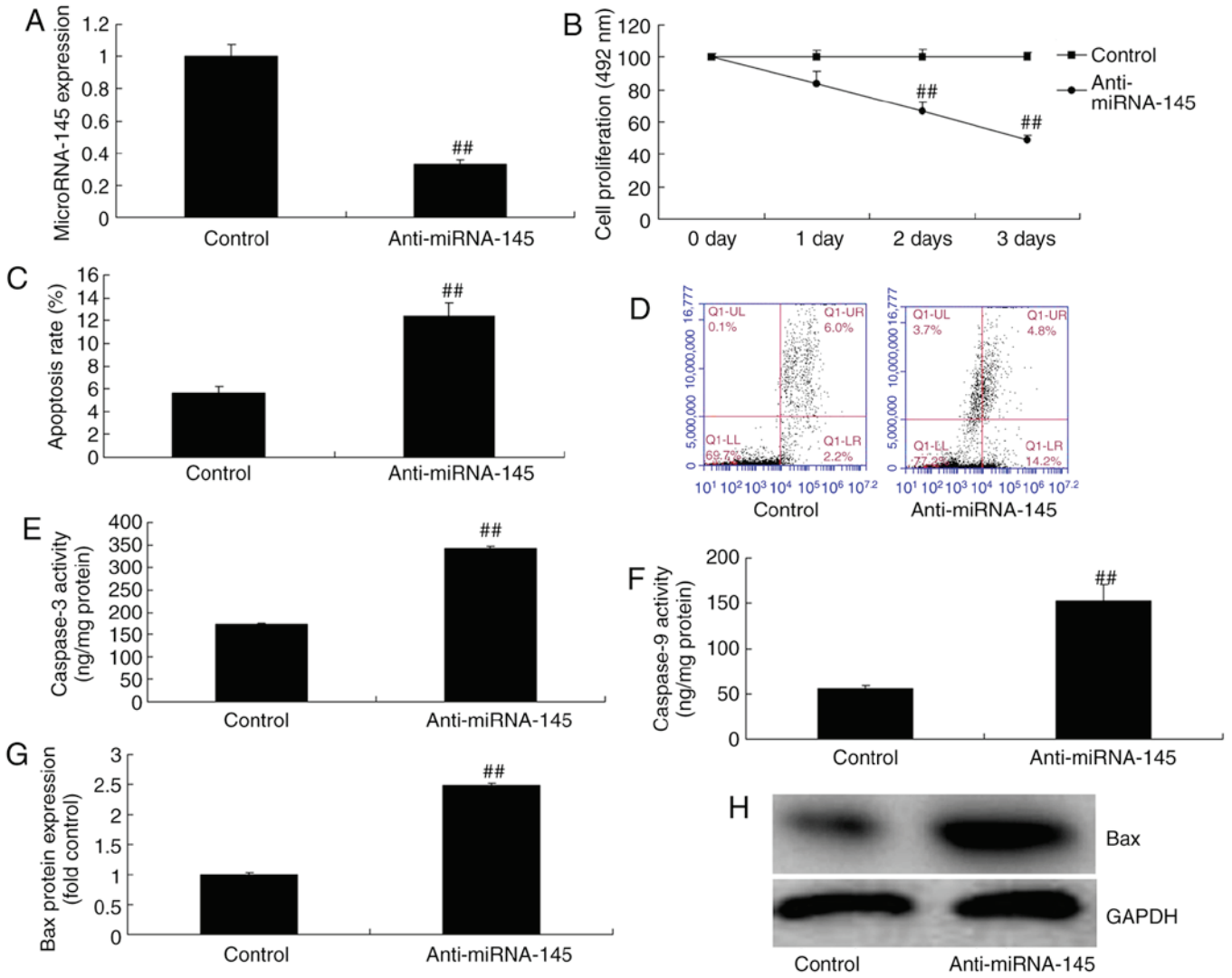

Figure 2. Downregulation of miRNA-145 increases cardiac cell apoptosis in an *in vitro* model of acute myocardial infarction. Quantitative analysis of (A) miRNA-145 expression and (B) cell proliferation. (C) Quantitative analysis and (D) representative image of apoptosis rate detected via flow cytometry. Quantitative analysis of (E) caspase-3 and (F) caspase-9 activities. (G) Quantitative analysis and (H) representative image of Bax protein expression detected via western blotting. ##P<0.01 vs. control group. miRNA, microRNA; control, control group; anti-miRNA-145, miRNA-145 downregulated group. Bax, B cell lymphoma 2 associated apoptosis regulator.

present study downregulated miRNA-145 expression levels using anti-miRNA-145 inhibitor. As presented in Fig. 2A, anti-miRNA-145 mimics decreased miRNA-145 expression, compared with control group. Downregulation of miRNA-145 inhibited cell proliferation and increased apoptosis rate, compared with control group (Fig. 2B-D). Downregulation of miRNA-145 additionally promoted caspase-3 and -9 activities, and induced Bax protein expression, compared with control group (Fig. 2E-H).

Downregulation of miRNA-145 suppresses autophagy in an in vitro model of AMI. To validate the mechanism of miRNA-145 on apoptosis in AMI, the present study measured the alterations of autophagy. Downregulation of miRNA-145 suppressed LC3 and ATG5 protein expression compared with control group (Fig. 3A-C). Immunofluorescent staining demonstrated that downregulation of miRNA-145 suppressed LC3 protein expression compared with control group (Fig. 3D).

Downregulation of miRNA-145 suppresses p-Akt3 and p-mTOR protein expression in an in vitro model of AMI. Bioinformatics software (www.targetscan.org) was used to analyze the targeted association between miRNA-145 and Akt3. As presented in Fig. 4A, Akt3 was predicted to be the target gene of miRNA-145. The results of the western blotting demonstrated that downregulation of miRNA-145 suppressed p-Akt3 and p-mTOR protein expression, compared with control group (Fig. 4B-D). The immunofluorescent staining results presented in Fig. 5 revealed that downregulation of miRNA-145 suppressed p-Akt3 protein expression, compared with control group.

Overexpression of miRNA-145 decreases cardiac cell apoptosis in an in vitro model of AMI. To demonstrate the function of miRNA-145 in cardiac cell apoptosis, the present study used miRNA-145 mimics to increase miRNA-145 expression. As presented in Fig. 6A, miRNA-145 mimics increased miRNA-145 expression, compared with control

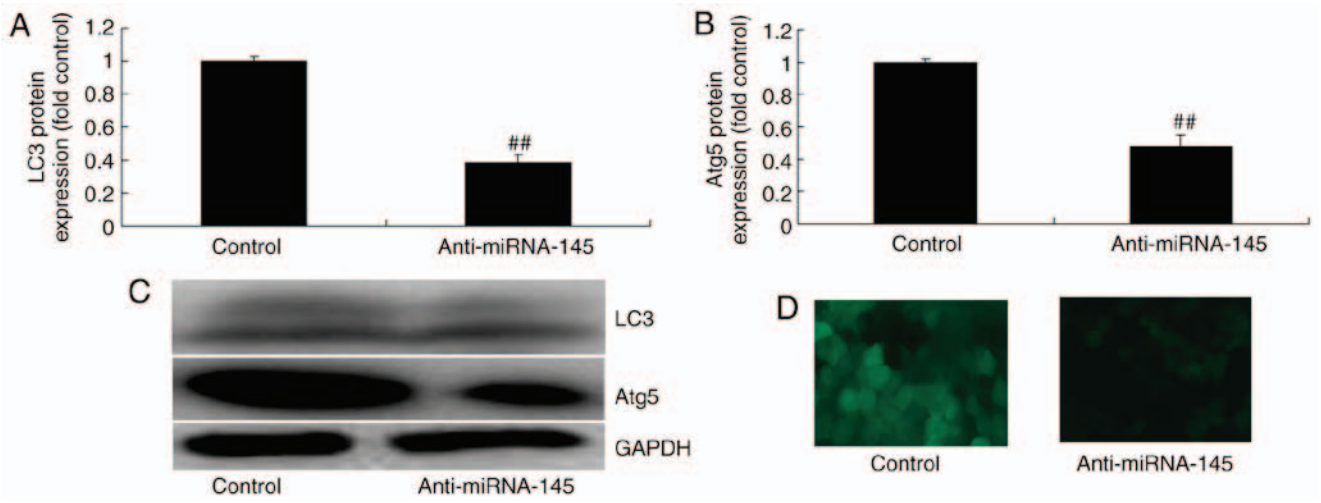

Figure 3. Downregulation of miRNA-145 suppresses autophagy in an *in vitro* model of acute myocardial infarction. Quantitative representation of (A) LC3, (B) Atg5 protein expression levels and (C) representative image, detected via western blotting. (D) Immunofluorescent staining for LC3 protein expression. ##P<0.01 vs. control group. miRNA, microRNA; control, control group; anti-miRNA-145, miRNA-145 downregulated group; LC3, microtubule associated protein 1 light chain 3; Atg5, autophagy protein 5.

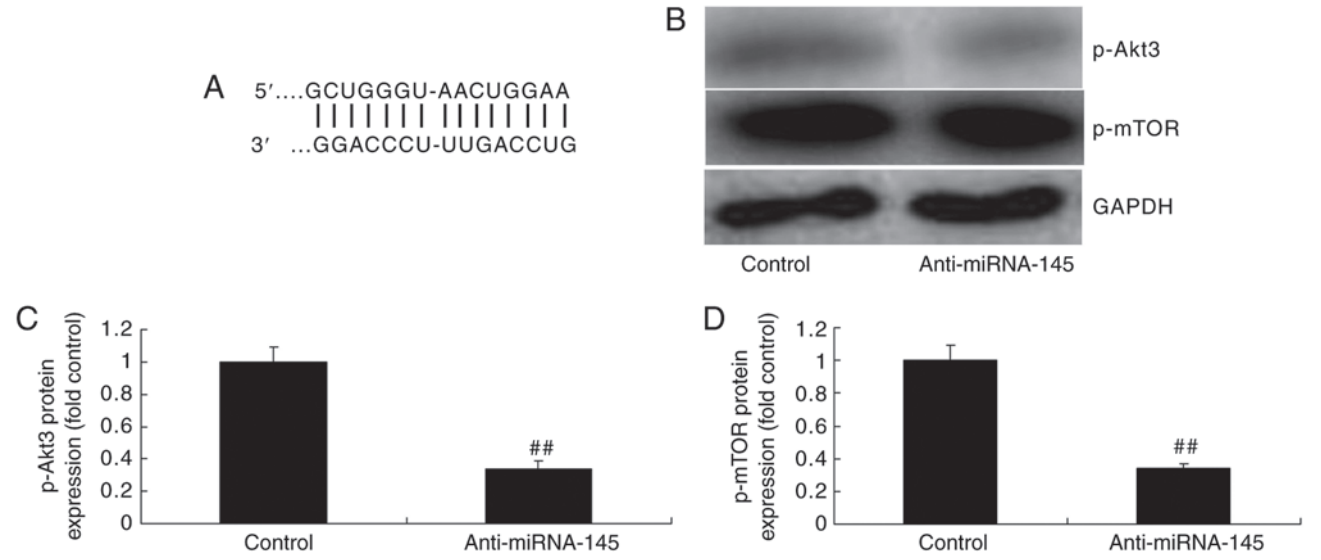

Figure 4. Downregulation of miRNA-145 suppresses p-Akt3 and p-mTOR protein expression in an *in vitro* model of acute myocardial infarction. (A) Bioinformatics software analysis identified the targeted association between miRNA-145 and Akt3. (B) Representative image and quantification of (C) p-Akt3 and (D) p-mTOR protein expression levels detected via western blotting. ##P<0.01 vs. control group. miRNA, microRNA; control, control group; anti-miRNA-145, miRNA-145 downregulated group; p, phosphorylated; Akt3, RAC-γ serine/threonine-protein kinase; mTOR, mechanistic target of rapamycin.

group. Overexpression of miRNA-145 promoted cell proliferation, and decreased cardiac cell apoptosis, compared with control group (Fig. 6B-D). The overexpression of miRNA-145 reduced Bax protein expression and inhibited caspase-3/9 activities compared with control group (Fig. 6E-H).

Overexpression of miRNA-145 induces p-Akt3 and p-mTOR protein expression and promotes autophagy in an in vitro model of AMI. The overexpression of miRNA-145 promoted LC3 and AGT 5 protein expression, compared with control group (Fig 7A-C). Immunofluorescent staining indicated that the overexpression of miRNA-145 promoted LC3 protein expression compared with control group (Fig. 7D). In addition, it was demonstrated that p-Akt3 and p-mTOR protein expression levels were increased, compared with control group (Fig. 7E-G).

Inhibition of Akt3 suppresses the effects of miRNA-145 upregulation on cell apoptosis in an in vitro model of AMI. The present study next explored the function of Akt3 in the effects of miRNA-145 upregulation on cell apoptosis. As presented in Fig. 8A-C, administration of 1 nM Akt3 inhibitor GSK2110183 following miRNA-145 upregulation, suppressed p-Akt3 and p-mTOR protein expression, compared with upregulated miRNA-145 group. Furthermore, the inhibition of Akt3 following miRNA-145 upregulation suppressed LC3 and AGT5 protein expression,

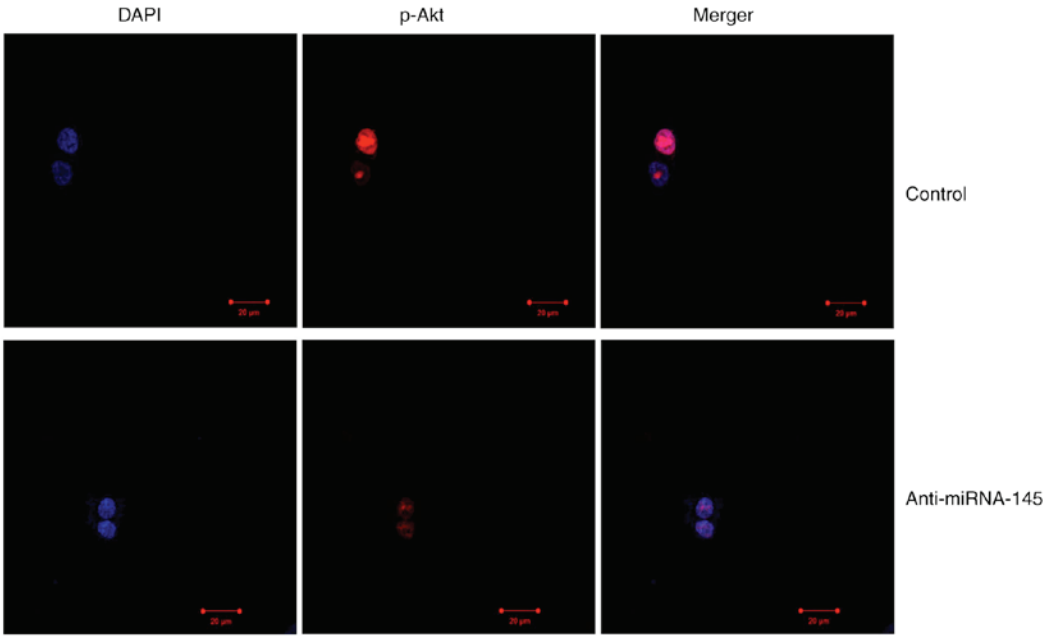

Figure 5. Downregulation of miRNA-145 suppresses p-Akt3 protein expression in an *in vitro* model of AMI. Immunofluorescent staining revealed that p-Akt3 protein expression was decreased in AMI. Magnification, x10. AMI, acute myocardial infarction; miRNA, microRNA; control, control group; anti-miRNA-145, miRNA-145 downregulated group; p, phosphorylated; Akt3, RAC-γ serine/threonine-protein kinase.

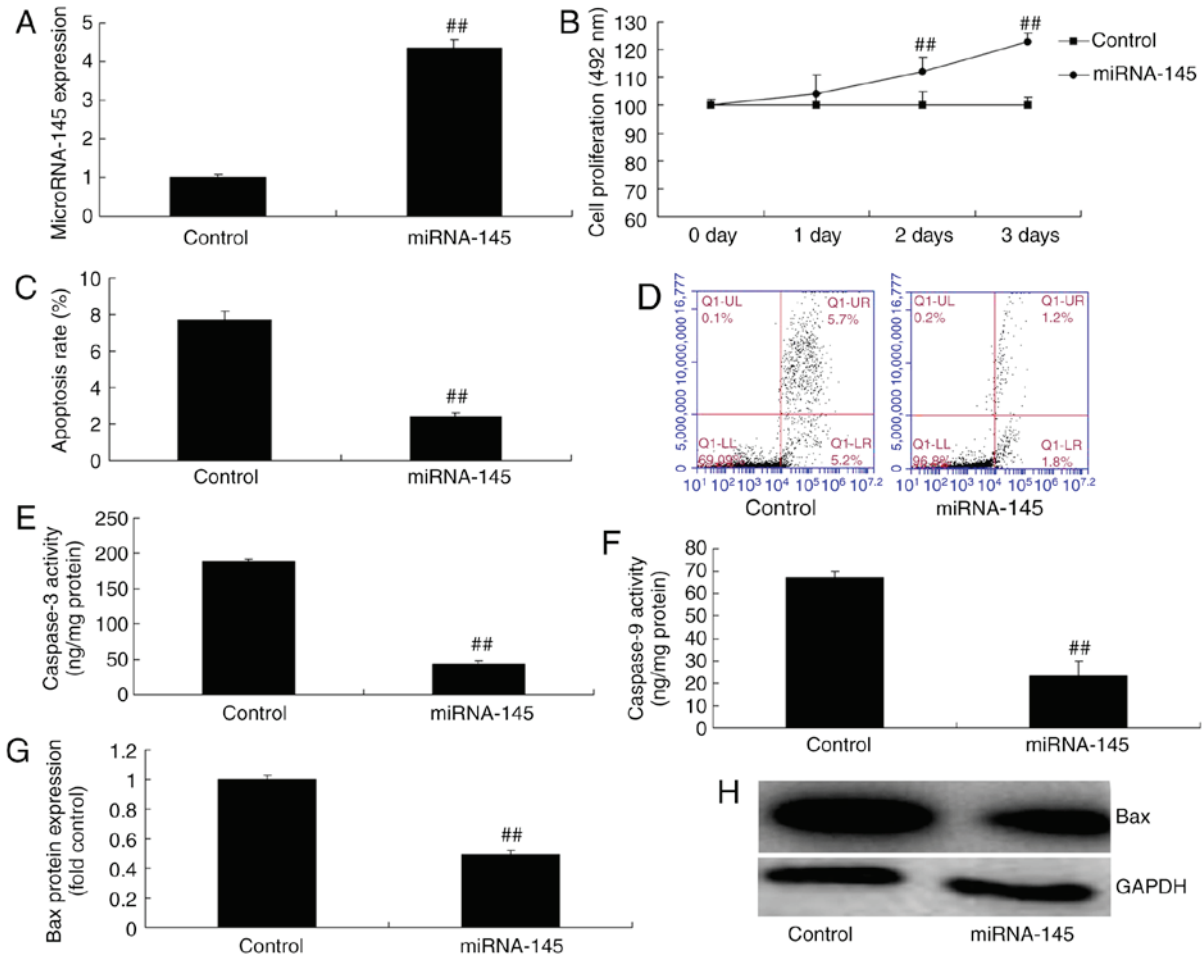

Figure 6. Overexpression of miRNA-145 decreases cardiac cell apoptosis in an *in vitro* model of acute myocardial infarction. Quantitative analysis of (A) miRNA-145 expression and (B) cell proliferation. (C) Quantitative analysis and (D) representative image of apoptosis rate detected via flow cytometry. Quantitative analysis of (E) caspase-3 and (F) caspase-9 activities. (G) Quantitative analysis and (H) representative image of Bax protein expression detected via western blotting. $^{\#\#}$P<0.01 vs. control group. miRNA, microRNA; miRNA-145, miRNA-145 overexpression group; control, control group; Bax, B cell lymphoma 2 associated apoptosis regulator.

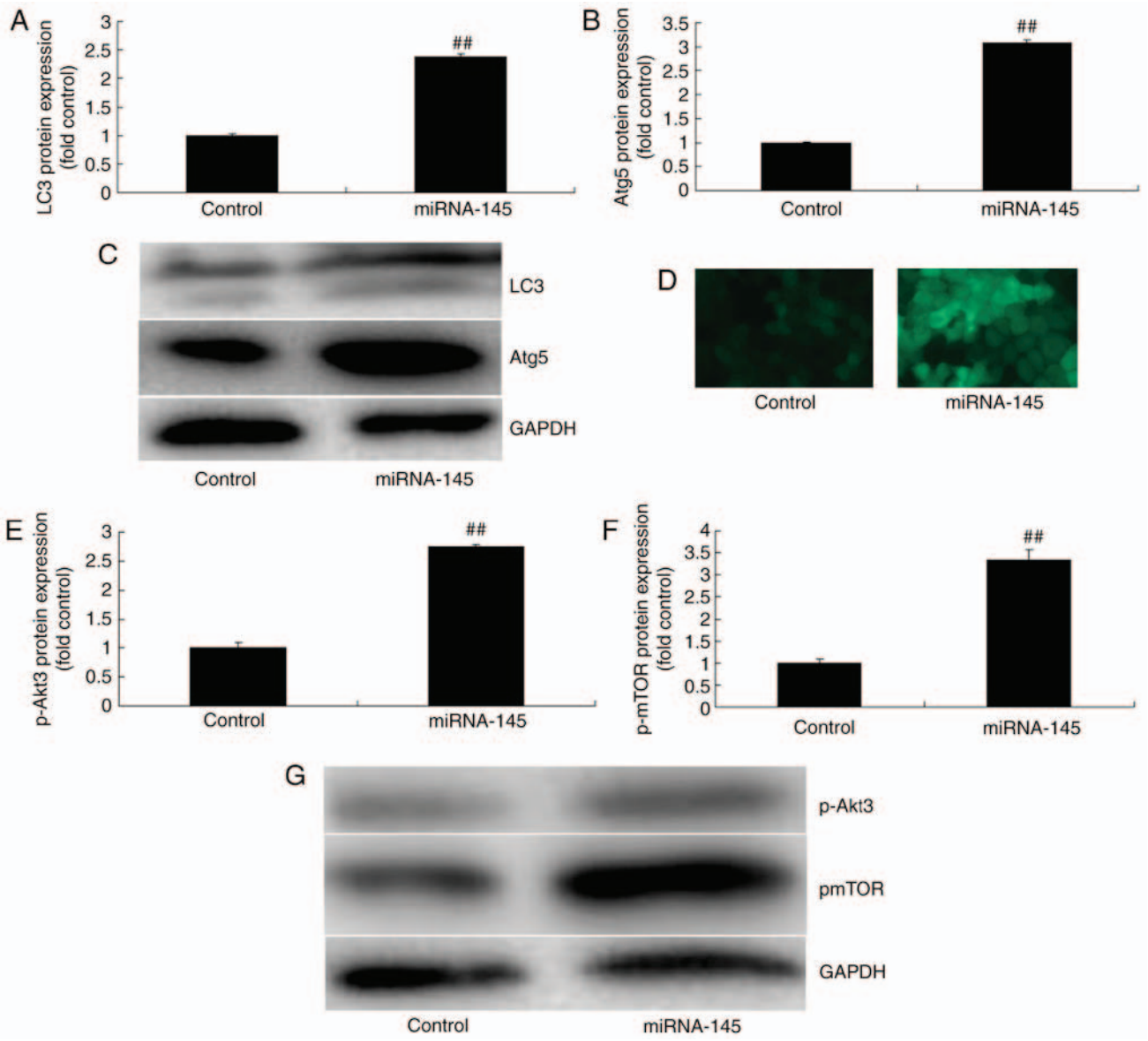

Figure 7. Overexpression of miRNA-145 induces autophagy and increases p-Akt3 and p-mTOR protein expression in an *in vitro* model of acute myocardial infarction. Quantitative representation of (A) LC3, (B) Atg5 protein expression levels and (C) representative image, detected via western blotting. (D) Immunofluorescent staining for LC3 protein expression. Quantitative analysis of (E) p-Akt3, (F) p-mTOR protein expression levels and (G) representative image, detected via western blotting. $^{##}$P<0.01 vs. control group. miRNA, microRNA; miRNA-145, miRNA-145 overexpression group; control, control group; LC3, microtubule associated protein 1 light chain 3; Atg5, autophagy protein 5; p, phosphorylated; Akt3, RAC-γ serine/threonine-protein kinase; mTOR, mechanistic target of rapamycin.

compared with upregulated miRNA-145 group (Fig. 8D-G). The effects of miRNA-145 upregulation on cell proliferation, cardiac cell apoptosis and Bax protein expression, in addition to caspase-3/9 activities, were reversed by Akt3 inhibitor, compared with upregulated miRNA-145 group (Fig. 9).

Lysosomal inhibitors inhibit the effects of miRNA-145 upregulation on cell apoptosis in an in vitro model of AMI. Exposure to a total of 5 μM lysosomal inhibitor chloroquine diphosphate following miRNA-145 upregulation increased Bax protein expression levels compared with miRNA-145 upregulated group (Fig. 10A-C). In addition, chloroquine diphosphate reduced cell growth, increased cardiac cell apoptosis, and promoted caspase-3 and caspase-9 activities, compared with miRNA-145 upregulated group (Fig. 10D-H).

Discussion

AMI is the primary cause of coronary heart disease-associated mortalities (1). Early thrombolytic therapy or percutaneous coronary intervention has been adopted to recover blood perfusion in the ischemic site. This method effectively rescues the injured myocardium (1) and improves myocardial ischemia and necrosis (2). However, adverse effects include partial myocardial cell apoptosis and loss of heart function. These effects are termed ischemia reperfusion injury (2). At present, the potential cellular mechanism leading to ischemia reperfusion injury remains to be fully

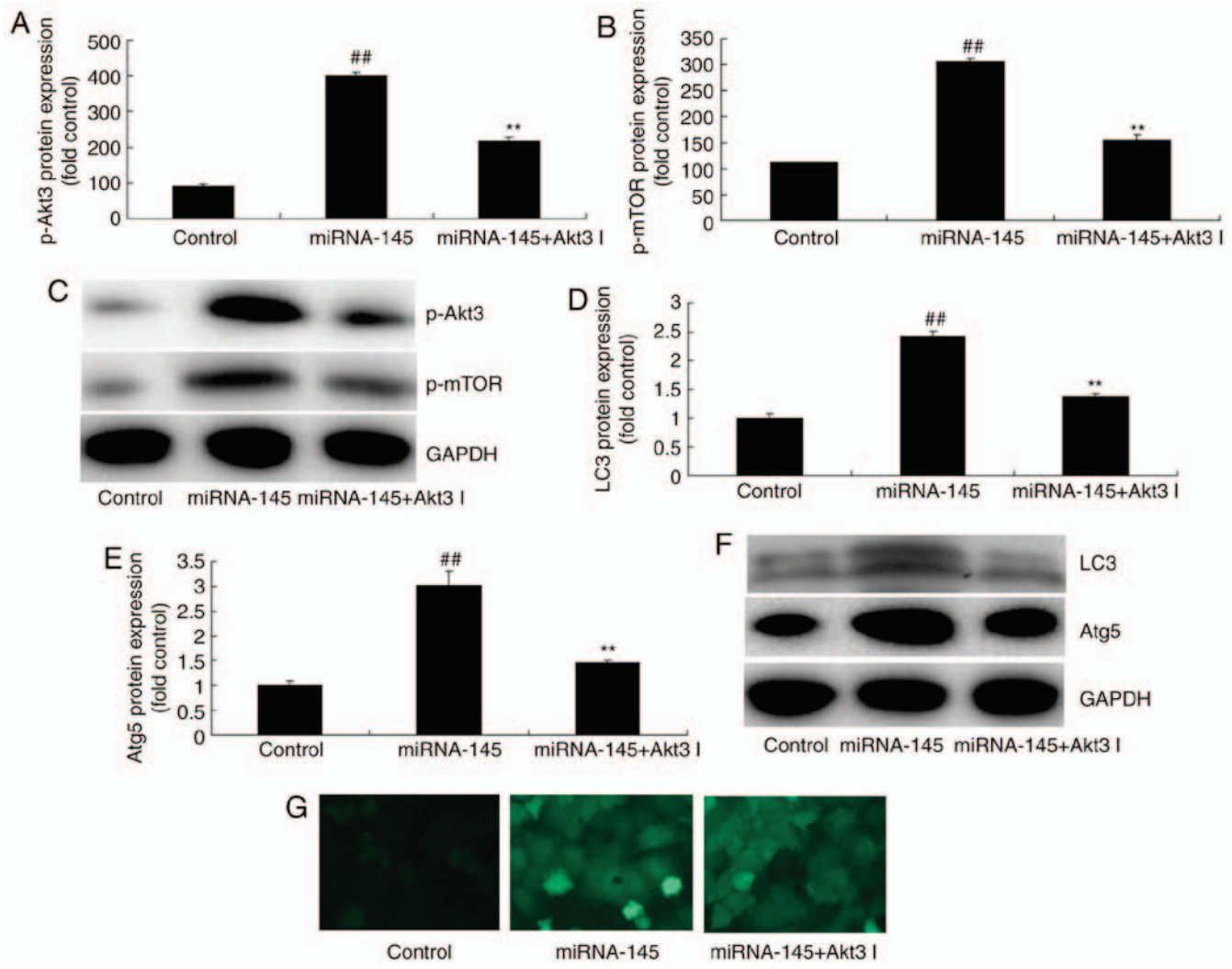

Figure 8. Inhibition of Akt3 suppresses the effects of miRNA-145 upregulation on cell apoptosis in an *in vitro* model of acute myocardial infarction. Quantification of (A) p-Akt3, (B) p-mTOR protein expression levels and (C) representative image, detected via western blotting. Quantification of (D) LC3, (E) Atg5 protein expression levels and (F) representative image, detected via western blotting. (G) Immunofluorescent staining for LC3 protein expression levels. $^{\#\#}$P<0.01 vs. control group; **P<0.01 vs. miRNA-145 overexpression group. miRNA, microRNA; control, control group; miRNA-145, miRNA-145 overexpression group; miRNA-145 + Akt3 I, miRNA-145 overexpression and Akt3 inhibitor group; LC3, microtubule associated protein 1 light chain 3; Atg5, autophagy protein 5; p, phosphorylated; Akt3, RAC-γ serine/threonine-protein kinase; mTOR, mechanistic target of rapamycin.

elucidated (3). The present study observed that miRNA-145 expression was downregulated in the AMI rat model, compared with control group.

miRNA is a highly conserved small non-coding RNA molecule (17) that regulates mRNA gene expression through complementary base pairing with mRNA (17). miRNA is intracellular RNA (17) and may regulate the post-transcription expression levels of multiple mRNAs. Therefore, it exhibits the potential to act as a useful therapeutic target. Numerous studies have been conducted researching the pathogenesis of CVD (18). Furthermore, miRNA alterations have been demonstrated to be involved in angiogenesis, myocardial hypertrophy, heart failure and myocardial fibrosis (18). The present study demonstrated that the downregulation of miRNA-145 increased cardiac cell apoptosis in an *in vitro* model of AMI. In accordance with the findings, Zhang *et al* (19) additionally suggests that miRNA-145 levels decrease in AMI.

Autophagy is commonly seen in acute and chronic myocardial ischemia and heart failure. It has previously been demonstrated that autophagy is markedly upregulated in ischemia reperfusion myocardial cells (20). Cell autophagy is the process by which lysosomes in the eukaryote degrade the damaged substances in the cell (21). In this process, various damaged proteins or organelles are consumed by the autophagosome with a bilayer structure (21). They are sent to the lysosome (animal) or vacuole (yeast and plant) for degradation, or are recycled (21). The results of the present study revealed that downregulation of miRNA-145 suppressed autophagy in an *in vitro* model of AMI. Higashi *et al* (22) suggests that miRNA-145 repairs infarcted myocardium by accelerating cardiomyocyte autophagy (21).

PI3K activates the serine/threonine Akt. Akt leads to the phosphorylation of serine/threonine mTOR via numerous regulators (23). mTOR is a serine/threonine protein kinase (23), highly conserved from fungus to mammal. The primary effect of mTOR is to regulate the cell cycle, cell growth and proliferation (24). Therefore, mTOR in mammals maintains a constant state of activation. This results in a

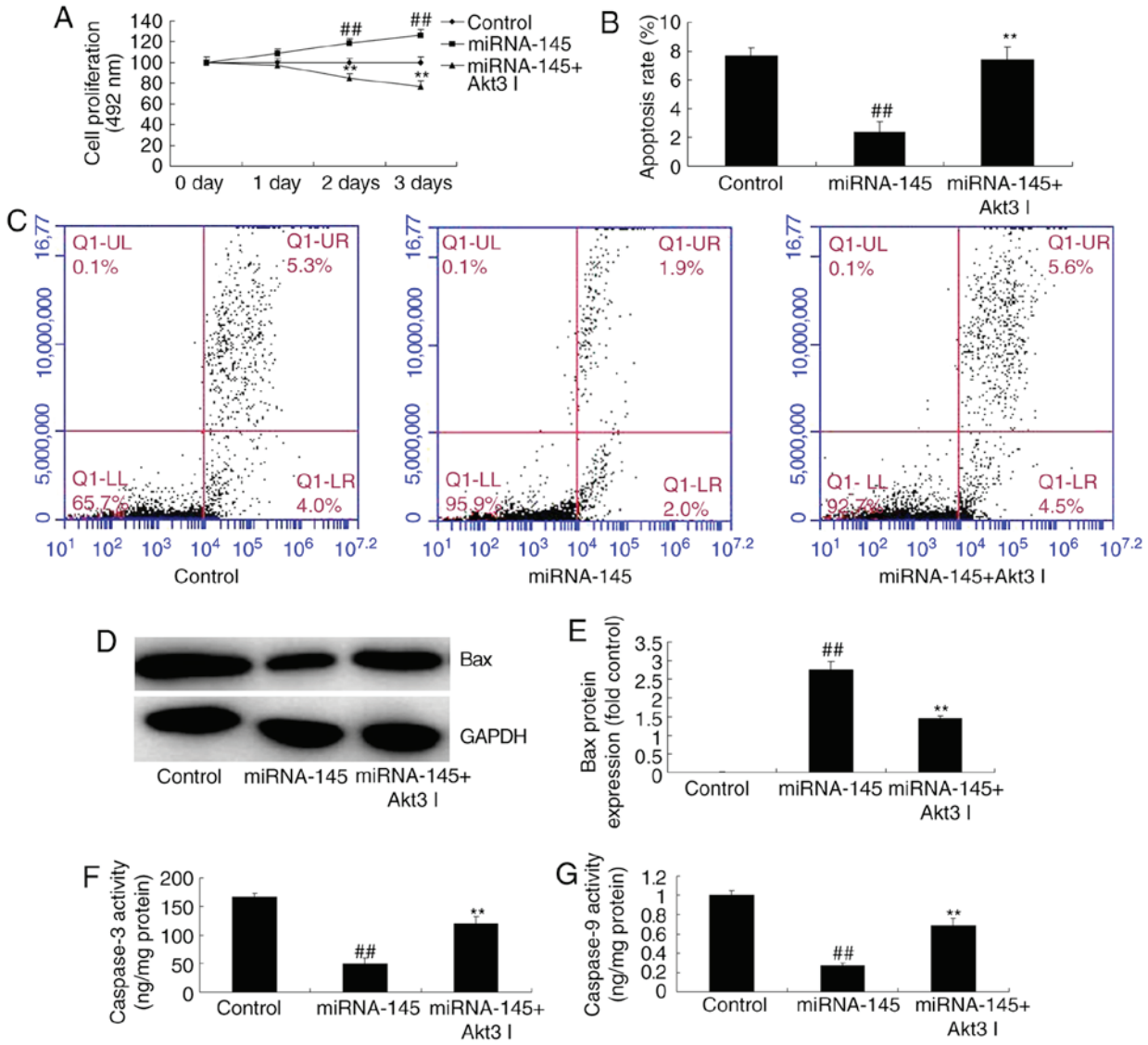

Figure 9. Inhibition of Akt3 inhibits the effects of miRNA-145 upregulation on cell apoptosis in an *in vitro* model of acute myocardial infarction. (A) Cell proliferation detected via MTT assay. (B) Quantitative analysis and (C) representative image of apoptosis rate detected by flow cytometry. (D) Representative image and (E) quantitative analysis of Bax protein expression. Quantitative analysis of (F) caspase-3 and (G) caspase-9 activities detected via western blotting. ##P<0.01 vs. control group; **P<0.01 vs. miRNA-145 overexpression group. miRNA, microRNA; control, control group; miRNA-145, miRNA-145 overexpression group; miRNA-145 + Akt3 I, miRNA-145 overexpression and Akt3 inhibitor group; Bax, B cell lymphoma 2 associated apoptosis regulator.

dynamic balance between cell growth and metabolism. Research has verified that mTOR has a role as an active switch in regulatory cell autophagy. It senses the alterations of multiple intracellular and extracellular signals. In addition to this, it activates or inhibits the rate of autophagy (24). Subsequently, it enhances cell adaptability to environmental stress (24). The present study observed that the downregulation of miRNA-145 suppressed p-Akt3 and p-mTOR protein expression. Furthermore, the inhibition of Akt3 decreased the effects of miRNA-145 upregulation on cell apoptosis. The lysosomal inhibitor chloroquine diphosphate inhibited the effects of miRNA-145 upregulation on autophagy to adjust cell apoptosis, in an *in vitro* model of AMI (Fig. 11). Zhou *et al* (25) reported that an increase in miRNA-145 inhibits the proliferation and invasion of invasive pituitary adenoma cells through AKT3/mTOR signaling pathway *in vivo* and *in vitro* (25).

In conclusion, the results of the present study demonstrated that miRNA-145 inhibited myocardial infarction-induced apoptosis by induction of autophagy via the Akt3/mTOR signaling pathway, *in vivo* and *in vitro*. This finding increases the understanding of miRNA in the field of molecular biology research, and will potentially be useful for treating myocardial infarction patients in the future. However, further analysis and larger samples are necessary in order to validate the results.

Acknowledgements

Not applicable.

Funding

No funding was received.

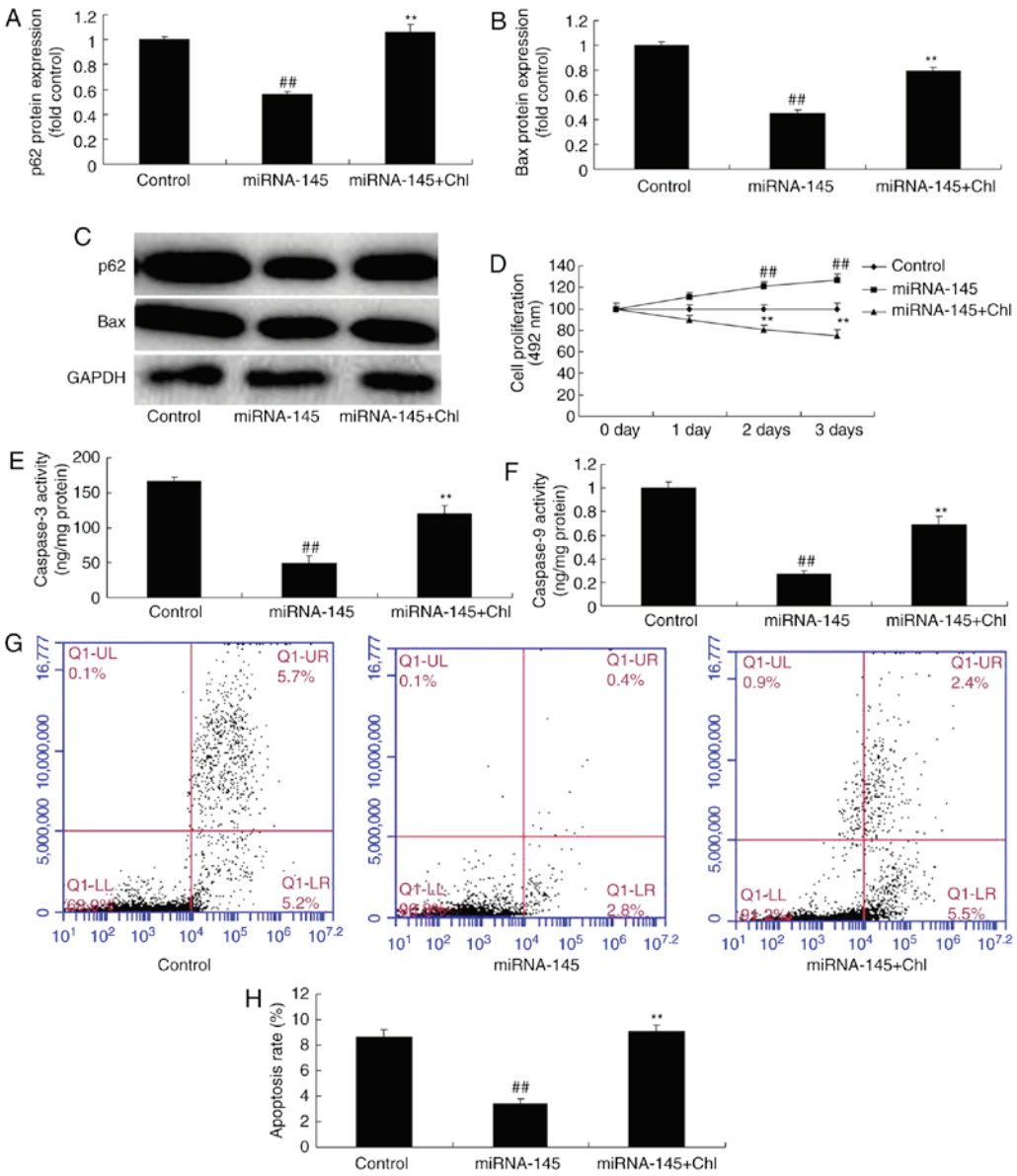

Figure 10. Lysosomal inhibitor inhibits effects of miRNA-145 upregulation on cell apoptosis in an *in vitro* model of AMI. Quantitative analysis of (A) P62, (B) Bax protein expression levels, and (C) representative image, detected via western blotting. (D) Cell proliferation detected via MTT assay. Quantitative analysis of (E) caspase-3 and (F) caspase -9 activities. (G) Representative image and (H) quantitative analysis of apoptosis rate detected via flow cytometry. $^{\#\#}$P<0.01 vs. control group; **P<0.01 vs. miRNA-145 overexpression group. miRNA, microRNA; control, control group; miRNA-145, miRNA-145 overexpression group; miRNA-145 + Chl, miRNA-145 overexpression and chloroquine diphosphate group; Bax, B cell lymphoma 2 associated apoptosis regulator.

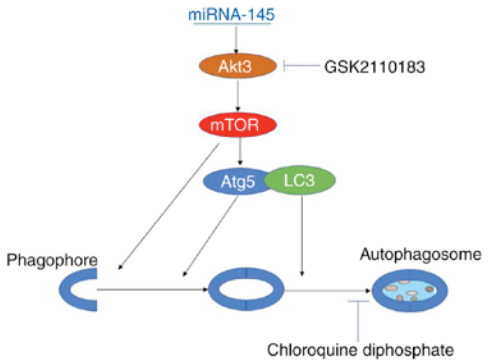

Figure 11. miRNA-145 inhibits myocardial infarction-induced apoptosis through autophagy by Akt3/mTOR signaling pathway *in vivo* and *in vitro*. miRNA, microRNA; LC3, microtubule associated protein 1 light chain 3; Atg5, autophagy protein 5; Akt3, RAC-γ serine/threonine-protein kinase; mTOR, mechanistic target of rapamycin.

Availability of data and materials

The analyzed data sets generated during the study are available from the corresponding author on reasonable request.

Authors' contributions

LY designed the experiment; NG, YC, SZ, JW, FL, YW and XC performed the experiments; LY analyzed the data and wrote the manuscript.

Ethics approval and consent to participate

All animal experiments were approved by the Ethics Committee of Cangzhou Central Hospital (Cangzhou, China).

Patient consent for publication

Not applicable.

Competing interests

The authors declare that they have no competing interests.

References

1. Pöss J, Köster J, Fuernau G, Eitel I, de Waha S, Ouarrak T, Lassus J, Harjola VP, Zeymer U, Thiele H and Desch S: Risk stratification for patients in cardiogenic shock after acute myocardial infarction. J Am Coll Cardiol 69: 1913-1920, 2017.
2. Myojo M, Ando J, Uehara M, Daimon M, Watanabe M and Komuro I: Feasibility of extracorporeal shock wave myocardial revascularization therapy for post-acute myocardial infarction patients and refractory angina pectoris patients. Int Heart J 58: 185-190, 2017.
3. Yurdakul S and Aytekin S: Left atrial mechanical functions in patients with anterior myocardial infarction: A velocity vector imaging-based study. Kardiol Pol 71: 1266-1272, 2013.
4. Erkol A, Oduncu V, Turan B, Kılıçgedik A, Sırma D, Gözübüyük G, Karabay CY, Guler A, Dündar C, Tigen K, *et al*: The value of plasma D-dimer level on admission in predicting no-reflow after primary percutaneous coronary intervention and long-term prognosis in patients with acute ST segment elevation myocardial infarction. J Thromb Thrombolysis 38: 339-347, 2014.
5. Liu Z, Ye P, Wang S, Wu J, Sun Y, Zhang A, Ren L, Cheng C, Huang X, Wang K, *et al*: MicroRNA-150 protects the heart from injury by inhibiting monocyte accumulation in a mouse model of acute myocardial infarction. Circ Cardiovasc Genet 8: 11-20, 2015.
6. Boon RA and Dimmeler S: MicroRNAs in myocardial infarction. Nat Rev Cardiol 12: 135-142, 2015.
7. Bronze-da-Rocha E: MicroRNAs expression profiles in cardiovascular diseases. Biomed Res Int 2014: 985408, 2014.
8. Guo X, Jiang H, Yang J, Chen J, Yang J, Ding JW, Li S, Wu H and Ding HS: Radioprotective 105 kDa protein attenuates ischemia/reperfusion-induced myocardial apoptosis and autophagy by inhibiting the activation of the TLR4/NF-κB signaling pathway in rats. Int J Mol Med 38: 885-893, 2016.
9. Xia Y, Liu Y, Xia T, Li X, Huo C, Jia X, Wang L, Xu R, Wang N, Zhang M, *et al*: Activation of volume-sensitive Cl-channel mediates autophagy-related cell death in myocardial ischaemia/reperfusion injury. Oncotarget 7: 39345-39362, 2016.
10. Shao H, Yang L, Wang L, Tang B, Wang J and Li Q: MicroRNA-34a protect myocardial cells against ischemia-reperfusion injury through inhibiting autophagy via regulating TNFα expression. Biochem Cell Biol 96: 349-354, 2017.
11. Buss SJ, Riffel JH, Katus HA and Hardt SE: Augmentation of autophagy by mTOR-inhibition in myocardial infarction: When size matters. Autophagy 6: 304-306, 2010.
12. Hou S, Yin X, Wang Z, Zhang J, Yuan Q and Chen Z: Cardamonin attenuates lung carcinoma and promotes autophagy via targeting p53 and regulating mTOR. Eur J Pharmacol S0014-2999: 30466 2017.
13. Suhara T, Baba Y, Shimada BK, Higa JK and Matsui T: The mTOR signaling pathway in myocardial dysfunction in type 2 diabetes mellitus. Curr Diab Rep 17: 38, 2017.
14. Yao H, Han X and Han X: The cardioprotection of the insulin-mediated PI3K/Akt/mTOR signaling pathway. Am J Cardiovasc Drugs 14: 433-442, 2014.
15. Tanaka Y, Hosoyama T, Mikamo A, Kurazumi H, Nishimoto A, Ueno K, Shirasawa B and Hamano K: Hypoxic preconditioning of human cardiosphere-derived cell sheets enhances cellular functions via activation of the PI3K/Akt/mTOR/HIF-1α pathway. Am J Transl Res 9: 664-673, 2017.
16. Livak KJ and Schmittgen TD: Analysis of relative gene expression data using real-time quantitative PCR and the 2(-Delta Delta C(T)) method. Methods 25: 402-408, 2001.
17. Cortez-Dias N, Costa MC, Carrilho-Ferreira P, Silva D, Jorge C, Calisto C, Pessoa T, Robalo Martins S, de Sousa JC and da Silva PC: Circulating miR-122-5p/miR-133b ratio is a specific early prognostic biomarker in acute myocardial infarction. Circ J 81: 613, 2017.
18. Oyama Y, Bartman CM, Gile J and Eckle T: Circadian MicroRNAs in cardioprotection. Curr Pharm Des 23: 3723-3730, 2017.
19. Zhang M, Cheng YJ, Sara JD, Liu LJ, Liu LP, Zhao X and Gao H: Circulating MicroRNA-145 is associated with acute myocardial infarction and heart failure. Chin Med J (Engl) 130: 51-56, 2017.
20. Wang ZG, Li H, Huang Y, Li R, Wang XF, Yu LX, Guang XQ, Li L,Zhang HY and Zhao YZ: Nerve growth factor-induced Akt/mTOR activation protects the ischemic heart via restoring autophagic flux and attenuating ubiquitinated protein accumulation. Oncotarget 8: 5400-5413, 2017.
21. Peng YQ, Xiong D, Lin X, Cui RR, Xu F, Zhong JY, Zhu T, Wu F, Mao MZ, Liao XB and Yuan LQ: Oestrogen inhibits arterial calcification by promoting autophagy. Sci Rep 7: 3549, 2017.
22. Higashi K, Yamada Y, Minatoguchi S, Baba S, Iwasa M, Kanamori H, Kawasaki M, Nishigaki K, Takemura G and Kumazaki M: MicroRNA-145 repairs infarcted myocardium by accelerating cardiomyocyte autophagy. Am J Physiol Heart Circ Physiol 309: H1813-H1826, 2015.
23. Cui J, Zhang F, Wang Y, Liu J, Ming X, Hou J, Lv B, Fang S and Yu B: Macrophage migration inhibitory factor promotes cardiac stem cell proliferation and endothelial differentiation through the activation of the PI3K/Akt/mTOR and AMPK pathways. Int J Mol Med 37: 1299-1309, 2016.
24. Wu ST, Sun GH, Cha TL, Kao CC, Chang SY, Kuo SC and Way TD: CSC-3436 switched tamoxifen-induced autophagy to apoptosis through the inhibition of AMPK/mTOR pathway. J Biomed Sci 23: 60, 2016.
25. Zhou K, Fan YD, Wu PF, Duysenbi S, Feng ZH, Du GJ and Zhang TR: MicroRNA-145 inhibits the activation of the mTOR signaling pathway to suppress the proliferation and invasion of invasive pituitary adenoma cells by targeting AKT3 in vivo and in vitro. Onco Targets Ther 10: 1625-1635, 2017.